Inorganic Chemistry

Article

pubs.acs.org/IC

Near-Infrared Electrochromism in Electropolymerized Metallopolymeric Films of a Phen-1,4-diyl-Bridged Diruthenium Complex

Hai-Jing Nie and Yu-Wu Zhong*

Beijing National Laboratory for Molecular Sciences, CAS Key Laboratory of Photochemistry, Institute of Chemistry, Chinese Academy of Sciences, 2 Bei Yi Jie, Zhong Guan Cun, Beijing 100190, People's Republic of China

Supporting Information

ABSTRACT: A phen-1,4-diyl-bridged tris-bidentate diruthenium complex **3**$(PF_6)_2$, $[Ru_2(dpb)(vbpy)_4](PF_6)_2$, has been designed and prepared, where dpb is 1,4-di(pyrid-2-yl)benzene and vbpy is 5-vinyl-2,2′-bipyridine. Upon reductive electropolymerization, metallopolymeric thin films of this complex have been deposited on platinum and ITO glass electrode surfaces. These films display two well-separated redox couples at +0.16 and +0.60 V versus Ag/AgCl. In the mixed-valent state, these films display intense intervalence charge transfer absorptions around 1300 nm. The electrochromic behavior at this wavelength has been examined by spectroelectrochemical measurements and double-potential-step chronoamperometry. A highest optical contrast ratio of 41% at 1300 nm with a coloration efficiency of 200 cm^2/C has been achieved. The electrochromic behavior is highly dependent on the surface coverage. The highest contrast ratio was obtained with a film of 6.0×10^{-9} mol/cm^2. In addition, a monoruthenium complex **2**(PF_6), $[Ru(dpb)(vbpy)_2](PF_6)$, has been prepared and electropolymerized for a comparison study.

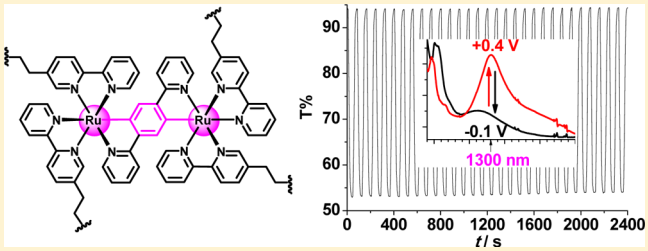

INTRODUCTION

Electrochromism refers to the reversible spectral and color changes of a material in response to an external electric stimulus.[1] Electrochromic materials are highly useful in a wide range of applications, such as smart windows/mirrors, electronic displays, dynamic camouflage, and information storage.[1] Typical electrochromic materials include inorganic metal oxides,[2] conducting polymers,[3] and molecular dyes.[1] Recently, transition metal complexes and coordination metallopolymers have received increasing interest as electrochromic materials.[4] Transition metal complexes often exhibit well-defined redox properties and intense charge transfer absorptions. More importantly, the absorption features of transition metal complexes are significantly dependent on the redox state of the material, which make them excellent candidates for electrochromic uses.[5]

For practical purposes, electrochromic materials must be deposited onto electrode surfaces as thin films. Routine film formation methods include vacuum deposition, spin-coating, drop-casting, layer-by-layer assembly, and electropolymerization, among others.[6] Vacuum deposition is not suitable for forming thin films of metallopolymers, because these materials are difficult to evaporate. Spin-coating and drop-casting are only useful for those with good solubility, e.g., the metallosupramolecular polymers reported by Higuchi, Kurth, and coworkers.[7] With appropriate molecular design, layer-by-layer assembled films with electrochromic functions have been constructed from pyridine or terpyridine-functionalized materials.[8] In comparison, electropolymerization is advantageous for forming thin films of metallopolymers, which only requires good solubility of monomers, and the polymeric films are *in situ* deposited on the electrode surfaces.[9] With appropriate polymerizable groups, such as thiophene,[10] pyrrole,[11] triarylamine derivatives,[12] and vinyl groups,[13] either oxidative or reductive polymerization of transition metal complexes have been reported to afford adhesive and electrochromic polymeric films.

Depending on the chemical structures and intrinsic properties of materials, the operating wavelength of electrochromism differs significantly. Materials showing electrochromism in the visible region have been frequently examined. In comparison, electrochromic materials and films concerning the spectra changes in the near-infrared (NIR) region are much less known,[14] although they are very useful in many civilian and military aspects.[15] In particular, NIR electrochromic films are potentially useful as variable optical attenuators for fiber telecommunications. The common optical fiber has the lowest energy loss at 1310 and 1550 nm,[16] and materials that display electrochromism at these two wavelengths are mostly desirable. Among known NIR electrochromic materials,[14] mixed-valence compounds have received much attention, displaying characteristic intervalence charge transfer (IVCT) transitions in the NIR region, and these transitions disappear in the homovalent states.

Received: August 15, 2014
Published: October 9, 2014

   dx.doi.org/10.1021/ic5019967 | *Inorg. Chem.* 2014, 53, 11316−11322

For instance, Wang and co-workers have elegantly demonstrated the electrochromism behavior of cross-linked polymeric films of diruthenium-dicarbonyl-dydrazido complexes,[16a−d] which display intense IVCT transitions around 1550 nm at the mixed-valent state. In addition, organic polymers with mixed-valent bis-triarylamine components have been shown to display promising NIR electrochromism by Liou and others.[17] In spite of these advances, new NIR electrochromic materials and films that can operate at the fiber-optic communication wavelengths with good contrast ratio and low operational voltages are still highly desirable.

We previously reported that bis-tridentate diruthenium complexes $[Ru_2(tpb)(tpy)_2]^{3+}$ (tpb = 1,2,4,5-tetra(pyrid-2-yl)benzene; tpy = 2,2′;6′,2″-terpyridine, Figure 1) and $[Ru_2(tppyr)(tpy)_2]^{3+}$ (1,3,6,8-tetra(pyrid-2-yl)pyrene) display promising NIR electrochromism due to the presence of intense IVCT transitions in the mixed-valent states.[18] The metallopolymeric films obtained via reductive electropolymerization of related vinyl-containing diruthenium complexes showed appealing NIR electrochromic behaviors with good contrast ratio and low switching voltage.[19] However, the operating wavelengths of these two films locate at 1160 and 2050 nm, respectively (Figure S1 in the Supporting Information, SI), which deviate significantly from the ideal wavelength for optical fiber communications (1310 or 1550 nm). We noticed that a similar tris-bidentate diruthenium complex, $[Ru_2(dpb)(bpy)_4]^{3+}$ (dpb = 1,4-di(pyrid-2-yl)benzene; bpy = 2,2′-bipyridine, Figure 1), possesses intense IVCT transition around 1300 nm in the mixed-valent state.[20] The change of the ruthenium coordination configuration from bis-tridentate to tris-bidentate leads to a dramatic shift of the energies of the IVCT transitions, which makes $[Ru_2(dpb)(bpy)_4]^{3+}$ a promising candidate for potential uses in optical fiber communications. We present in this Article the electropolymerization of a vinyl-containing analogous of $[Ru_2(dpb)(bpy)_4]^{3+}$, $\mathbf{3}(PF_6)_2$ (Scheme 1), and the electrochromic behavior at 1300 nm of the resulting metallopolymeric films.

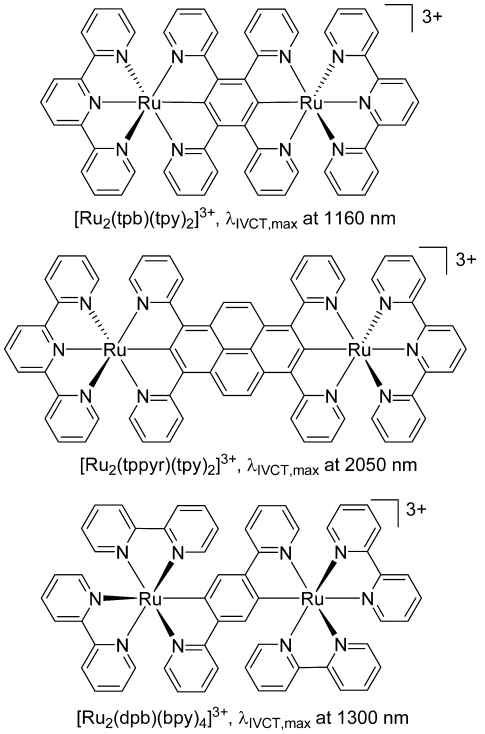

Figure 1. Mixed-valent diruthenium complexes with different IVCT absorption maxima.

RESULTS AND DISCUSSION

Complex $\mathbf{3}(PF_6)_2$ was designed as the monomer for the reductive electropolymerization (Scheme 1), where one vinyl group is appended to each bpy ligand of the $[Ru_2(dpb)(bpy)_4]$ framework. The reaction of dpb[20] with $[Ru(p\text{-cymene})Cl_2]_2$ in the presence of NaOH and KPF_6 afforded the diruthenium intermediate $\mathbf{1}(PF_6)_2$, $[Ru_2(dpb)(p\text{-cymene})_2(CH_3CN)_2](PF_6)_2$, in 50% yield. This intermediate is unstable in solution and used directly for the next transformation without full characterization. The MALDI-TOF mass spectrum of $\mathbf{1}(PF_6)_2$ shows signals at 890.3 and 702.2 D (Supporting Information Figure S2), corresponding to the $[Ru_2(dpb)(p\text{-cymene})_2(CH_3CN)](PF_6)$ and $[Ru_2(dpb)(p\text{-cymene})_2]$ fragment, respectively. The treatment of $\mathbf{1}(PF_6)_2$ with 5-vinyl-2,2′-bipyridine (vbpy)[21] gave two isolated complexes, $\mathbf{2}(PF_6)$ and $\mathbf{3}(PF_6)_2$, in 12% and 33% yield, respectively. Two possible reasons can be imagined to explain the isolation of the monoruthenium complex $\mathbf{2}(PF_6)$. One is that the diruthenium intermediate $\mathbf{1}(PF_6)_2$ was contaminated with a related monoruthenium intermediate. Another possibility is that

Scheme 1. Synthesis of $\mathbf{2}(PF_6)$ and $\mathbf{3}(PF_6)_2$

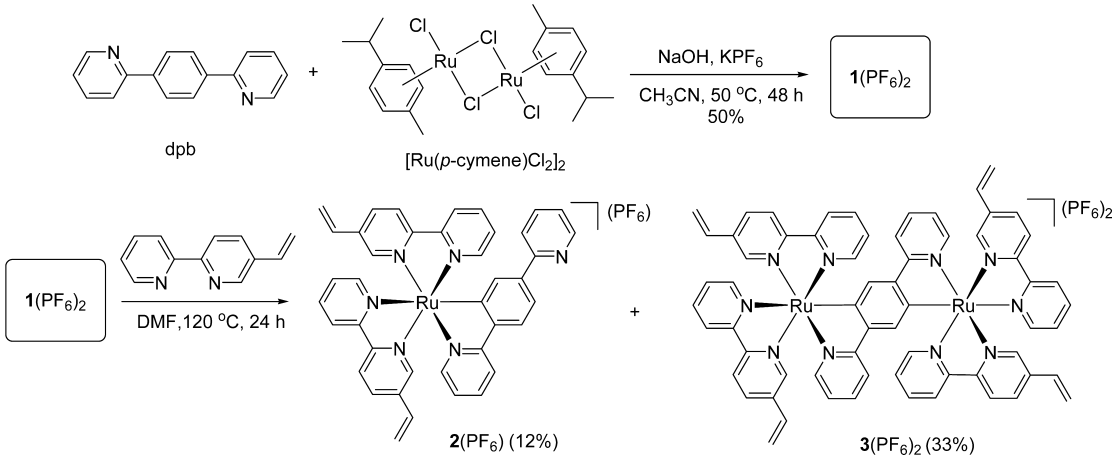

dx.doi.org/10.1021/ic5019967 | Inorg. Chem. 2014, 53, 11316−11322

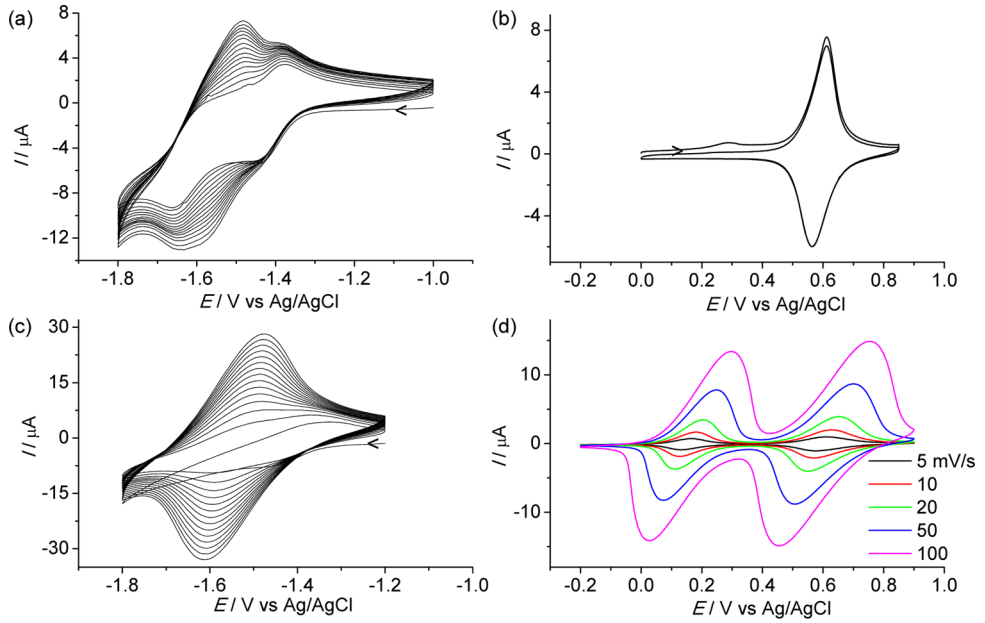

Figure 2. Reductive electropolymerization of (a) $\mathbf{2}(PF_6)$ and (c) $\mathbf{3}(PF_6)_2$ (0.5 mM in CH_3CN) on a disk platinum electrode (d = 2 mm) by 15 repeated potential scan cycles at 100 mV/s. (b) CV of the poly-$\mathbf{2}(PF_6)$/Pt film in 0.1 M Bu_4NClO_4/CH_2Cl_2 at 100 mV/s. (d) CVs of the poly-$\mathbf{3}(PF_6)_2$/Pt film in 0.1 M Bu_4NClO_4/CH_2Cl_2 at different scan rates (5, 10, 20, 50, and 100 mV/s, respectively).

some amounts of $\mathbf{1}(PF_6)_2$ were decomposed into a monoruthenium intermediate in the second step, which subsequently was transformed into $\mathbf{2}(PF_6)$. We did not attempt to fully address this issue at this stage and turned our attention into the following electropolymerization studies.

The MALDI-TOF mass spectrum of $\mathbf{2}(PF_6)$ shows the signal at 697.5 D (Supporting Information Figure S3), corresponding to the $[Ru(dpb)(vbpy)_2]$ fragment after the loss of the PF_6^- anion. The MALDI-TOF mass spectrum of $\mathbf{3}(PF_6)_2$ shows signals at 1306.2, 1162.2, and 697.8 D (Supporting Information Figure S4), corresponding to the $[Ru_2(dpb)(vbpy)_4](PF_6)$, $[Ru_2(dpb)(vbpy)_4]$, and $[Ru(dpb)(vbpy)_2]$ fragment, respectively.

The ^1H NMR signals corresponding to the vinyl groups of $\mathbf{2}(PF_6)$ can be clearly discerned around 5.3, 5.7, and 6.4 ppm from its NMR spectrum (Supporting Information Figure S5). Moreover, the ^1H NMR spectrum shows that three different isomers are present in the isolated sample of $\mathbf{2}(PF_6)$, judging from the signals at 5.3 ppm. Complex $\mathbf{3}(PF_6)_2$ shows ill-defined and broad ^1H NMR signals (Supporting Information Figure S6), possibly due to the contamination of partially oxidized paramagnetic species. In the presence of a small amount of aqueous hydrazine, the signals become more distinct. However, these signals are very complex, apparently due to the presence of many stereoisomers. These isomers are expected to make little difference to the energies of the IVCT transitions. The samples obtained were used for the following electropolymerization without further purification.

The electropolymerization was first examined on a platinum disk electrode. A clean platinum electrode was placed in a solution of $\mathbf{2}(PF_6)$ in 0.1 M Bu_4NClO_4/CH_3CN, and the potential was repeatedly scanned between −1.0 V and −1.8 V versus Ag/AgCl. The current increased gradually and continuously (Figure 2a), which indicated that the electropolymerization of $\mathbf{2}(PF_6)$ took place smoothly on the electrode surface. The mechanism of the polymerization is believed anionically initiated, followed subsequent radical−radical chain propagation.[13] Figure 2b shows the cyclic voltammogram (CV) of the obtained polymeric film at 100 mV/s in a clean electrolyte solution in CH_2Cl_2. A redox couple, attributed to the $Ru^{III/II}$ process,[20] at +0.59 V versus Ag/AgCl is observed for the thin film. The potential separation between the anodic and cathodic peak is 50 mV, which is slightly smaller relative to the theoretical value (59 mV) of a diffusion-controlled one-electron Nernstain wave. This is because the redox reaction of the thin film is confined on the electrode surface, instead of a diffusion-controlled process. For a surface-immobilized redox process, the peak potential separation should be theoretically zero. The relatively large peak separation of poly-$\mathbf{2}(PF_6)$ is possibly caused by the charge repulsion between neighboring metal complexes and the anion diffusion to compensate the charge changes upon redox reactions. This point will be further discussed below.

The cathodic CV scan of $\mathbf{2}(PF_6)$ shows two redox couples at −1.41 and −1.63 V, respectively, attributable to the reductions of two bipyridine ligands (Figure 2a). The cathodic scan of the diruthenium complex $\mathbf{3}(PF_6)_2$ shows less well-defined waves in the same region (Figure 2c), as a result of the reductions of four bipyridine ligands and the bridging ligand. However, the reductive electropolymerization of $\mathbf{3}(PF_6)_2$ proceeded equally well, and the polymerization efficiency is higher relative to $\mathbf{2}(PF_6)$. This can be reflected by the higher current of the poly-$\mathbf{3}(PF_6)_2$ film with respect to the poly-$\mathbf{2}(PF_6)$ film, which were both obtained via 15 cycles of potential scans and from the same concentration of corresponding monomers. This is reasonable because the diruthenium complex $\mathbf{3}(PF_6)_2$ has two more vinyl groups than the monoruthenium complex $\mathbf{2}(PF_6)$. A cross-linked polymeric network could be imagined for the poly-$\mathbf{3}(PF_6)_2$ film, considering the presence of multiple vinyl groups in this complex. Figure 2d shows the CVs of the poly-$\mathbf{3}(PF_6)_2$/Pt film in a clean electrolyte solution in CH_2Cl_2 at different scan rate (from 5 to 100 mV/s), which displays two stepwise and well-defined redox couples at +0.16 and +0.60 V. The previously reported prototype complex $[Ru_2(dpb)(bpy)_4]^{2+}$

dx.doi.org/10.1021/ic5019967 | Inorg. Chem. 2014, 53, 11316−11322

without vinyl groups possesses similar two stepwise redox couples at +0.18 and +0.62 V versus Ag/AgCl.[20] This indicates that the basic electrochemical properties of the dimetallic unit are retained after electropolymerization. The low $Ru^{III/II}$ potentials of these ruthenium complexes are a result of the presence of the electron-rich anionic phenyl ligand, which makes the oxidation of the ruthenium ion much easier relative to those of conventional ruthenium complexes.[20]

The anodic−cathodic peak potential separation of each redox couple of the poly-**3**$(PF_6)_2$ film is much larger with respect to that of poly-**2**(PF_6) film at the same scan rate. For instance, the peak separation of the poly-**3**$(PF_6)_2$ film is 270 mV at 100 mV/s. This peak potential separation decreases with decreasing scan rate. At the scan rate of 10 mV/s, the peak potential separation of each couple of the poly-**3**$(PF_6)_2$ film is 54 mV. The large peak potential separation of poly-**3**$(PF_6)_2$ film is partially because it has a higher surface coverage and thus lower electron transfer kinetics relative to the poly-**2**(PF_6) film. Another possible reason is that poly-**2**(PF_6) is essentially a linear polymer, while poly-**3**$(PF_6)_2$ is expected to have a cross-linked polymeric structure, which will suppress the counteranion diffusion accompanied by the interfacial electron transfer process. Both anodic and cathodic currents of poly-**2**(PF_6) and poly-**3**$(PF_6)_2$ films are linearly dependent on the scan rate, which is characteristic of redox processes confined on an electrode surface.

In order to examine the electrochromism of the above polymeric materials, thin films of **2**(PF_6) and **3**$(PF_6)_2$ were prepared by similar reductive electropolymerization on transparent indium−tin-oxide (ITO) glass electrodes (typical dimension of 0.8 cm × 2.0 cm). The obtained films were immersed in a clean electrolyte solution in CH_2Cl_2, and the absorption spectral changes were monitored upon stepwise oxidative electrolysis. When the potential was stepwisely applied to the poly-**2**(PF_6)/ITO film from +0.3 to +0.9 V versus Ag/AgCl, the metal-to-ligand-charge-transfer (MLCT) transitions in the visible region gradually decreased (Figure 3a). This process is reversible when the potential was reduced.

When the poly-**3**$(PF_6)_2$/ITO film was subjected to the stepwise oxidative electrolysis from −0.1 V to +0.4 V, the MLCT decreased as well. Concomitantly, intense IVCT absorptions[20] around 1300 nm appeared (Figure 3b). When the potential was further increased to +0.9 V, the IVCT absorptions decreased significantly (Figure 3c). The appearance of a new band around 650 nm was attributed to the ligand-to-metal-charge-transfer (LMCT) transitions.[20] These two step processes are totally reversible (see below). The film is wine, orange, and dark cyan at −0.1, +0.4, and +0.9 V, respectively (Supporting Information Figure S7).

The NIR electrochromism of the poly-**3**$(PF_6)_2$/ITO film was further investigated by double-potential-step chronoamperometry (−0.1 and +0.4 V vs Ag/AgCl) in conjunction with the monitoring of the transmittance (T%) changes of the film at 1300 nm (Figure 4). A contrast ratio (ΔT%) of 41% was achieved when a film with a surface coverage (Γ) of 6.0×10^{-9} mol/cm^2 was examined. The surface coverage was determined by using the equation $\Gamma = Q/nFA$, where Q is the charge under the $Ru^{III/II}$ wave of the polymeric films, n is the number of electrons per molecule reduced ($n = 1$), F is Faraday's constant (96 485 C/mol), and A is the area of the electrode in cm^2. The contrast ratio dropped 1.5% after 30 cycles of potential switching between −0.1 and +0.4 V (Figure 4), implying a good stability and steady electrochromic performance of the film.

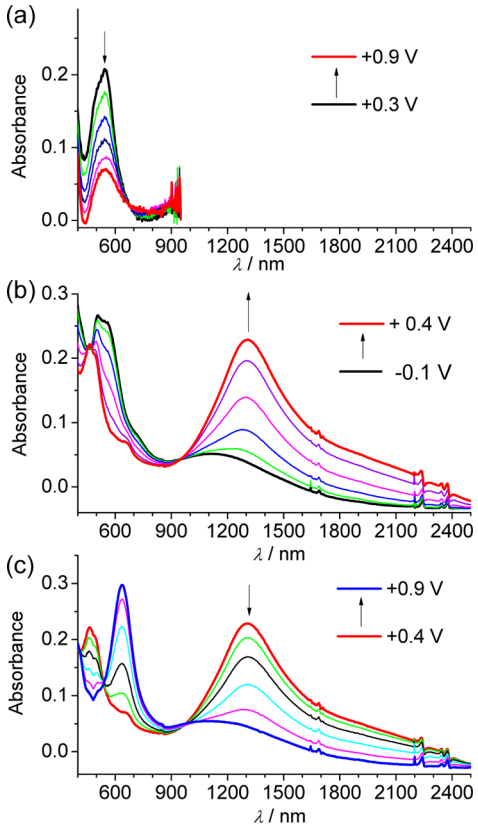

Figure 3. Absorption spectral changes of (a) poly-**2**(PF_6)/ITO film and (b,c) poly-**3**$(PF_6)_2$/ITO film in 0.1 M Bu_4NClO_4/CH_2Cl_2 recorded during oxidative spectroelectrochemical measurements. The applied potentials are referenced versus Ag/AgCl.

The response time for the contrast ratio to reach over 90% of its maximum of the above film is around 15−20 s for the oxidation and reverse reduction process, respectively. The slow response time is possibly caused the slow electron transfer kinetics of the film, as has been discussed in the above CV studies. The coloration efficiency (CE) at 1300 nm was calculated to be 200 cm^2/C according to the equation $CE(\lambda) = \Delta OD/Q_d$, where $\Delta OD = \log[T_b/T_c]$, OD is optical density, Q_d is the injected/ejected charge density (C/cm^2), and T_b and T_c are the transmittance in the bleached and colored states at indicated wavelength.

The electrochromism involving the second redox couple of the poly-**3**$(PF_6)_2$/ITO film has not been examined. The first redox couple has a relatively lower redox potential, which will be advantageous in reducing the operational voltage of practical devices. The second redox couple is associated with the absorption spectral changes at the same the wavelength, but has a much higher redox potential relative to the first one.

The surface coverage of the polymeric film makes a big difference to the electrochromic performance. By changing the electropolymerization duration, a series of poly-**3**$(PF_6)_2$/ITO films with the surface coverage ranging from 2.0×10^{-9} to 1.2×10^{-8} mol/cm^2 have been prepared. Figure 5 shows the plot of the contrast ratio at 1300 nm achieved for these films as a function of the surface coverage. The highest contrast ratio achieved is 41% with the film with $\Gamma = 6.0 \times 10^{-9}$ mol/cm^2. Films with a lower or higher surface coverage show poorer

dx.doi.org/10.1021/ic5019967 | Inorg. Chem. 2014, 53, 11316−11322

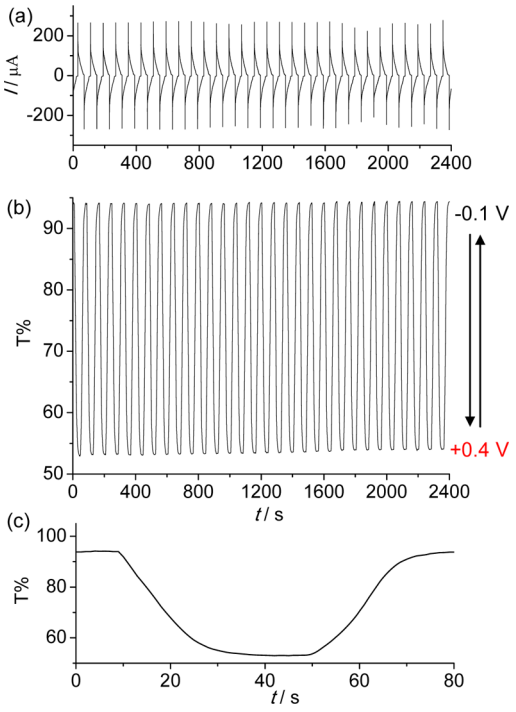

Figure 4. Thirty cycles of electrochromic switching of poly-$\mathbf{3}(PF_6)_2$/ITO film ($\Gamma = 6.0 \times 10^{-9}$ mol/cm^2) between −0.1 and +0.4 V versus Ag/AgCl with an interval of 20 s in 0.1 M Bu_4NClO_4/CH_2Cl_2. (a) Current assumption. (b and c) Transmittance changes monitored at 1300 nm as a function of time.

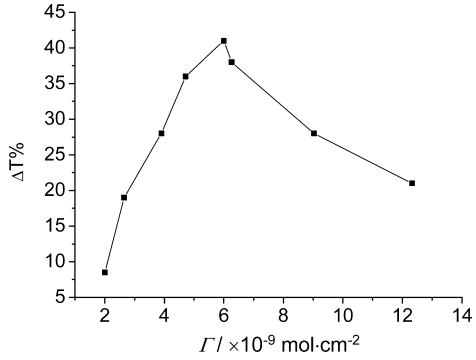

Figure 5. Plot of $\Delta T\%$ at 1300 nm vs Γ for the poly-$\mathbf{3}(PF_6)_2$/ITO film during the electrochromic switching between −0.1 and +0.4 V vs Ag/AgCl.

performance. However, films showing a lower contrast ratio, irrespective of the film thickness, have a relatively shorter response time. For instance, the poly-$\mathbf{3}(PF_6)_2$/ITO film with Γ of 2.7×10^{-9} mol/cm^2 shows a contrast ratio of 19% and a response time of 7 s (Supporting Information Figure S8a), and a thicker film with Γ of 1.2×10^{-8} mol/cm^2 shows a contrast ratio of 21% and a response time of 12 s (Supporting Information Figure S8b). The thick film with Γ of 1.2×10^{-8} mol/cm^2 has transmittance of 76% and 55% when the potential was applied at −0.1 and +0.4 V, respectively (Supporting Information Figure S8b). In comparison, the film with the optimal contrast ratio has transmittance of 94% and 53% at −0.1 and +0.4 V, respectively. This means that the drop in the contrast ratio with thicker films is mainly caused by the decrease of the transmittance at −0.1 V, which is likely a result of the molecular aggregation in thick films.

CONCLUSION

In conclusion, the phen-1,4-diyl-bridged tris-bidentate diruthenium complex $\mathbf{3}(PF_6)_2$ with four vinyl substituents has been designed and prepared. This complex was successfully deposited onto platinum and ITO glass electrodes by reductive electropolymerization. The resulting metallopolymeric films display promising electrochromism at the fiber-optic communication wavelength (1300 nm) with low operation potential. A highest contrast ratio of 41% with a coloration efficiency of 200 cm^2/C has been achieved. The films have good stability and show steady NIR electrochromic performance. They are potentially useful as variable optical attenuators for fiber telecommunications.

EXPERIMENTAL SECTION

Electrochemistry. All electrochemical experiment were carried out using a CHI 660D potentiostat. All measurements were carried out in 0.1 M Bu_4NClO_4 in CH_3CN or CH_2Cl_2 with a Ag/AgCl reference electrode. The working electrode was a homemade disk platinum electrode or a transparent ITO glass electrode (<10 Ω/square), and a platinum coil was used as the counter electrode. A three-compartment electrochemical cell was used in the electropolymerization experiments. In the case of using ITO as the working electrode, it was positioned parallel and opposite to the counter electrode.

Oxidative Spectroelectrochemical Measurements. Absorption spectra were recorded using a PerkinElmer Lambda 750 UV−vis−NIR spectrophotometer at room temperature in denoted solvents. The polymeric ITO film was immersed in 0.1 M Bu_4NClO_4/CH_2Cl_2 in a conventional cell, with a platinum wire as the counter electrode and Ag/AgCl in saturated aqueous NaCl solution as the reference electrode. The cell was put into the spectrophotometer to monitor the spectral changes upon stepwise oxidative electrolysis using a CHI 660D potentiostat.

Synthesis of $\mathbf{2}(PF_6)$ and $\mathbf{3}(PF_6)_2$. To a solution of 1,4-di(pyrid-2-yl)benzene (dpb, 32.0 mg, 0.14 mmol) in 10 mL dry CH_3CN were added $[Ru(p\text{-cymene})Cl_2]_2$ (100 mg, 0.17 mmol), KPF_6 (102 mg, 0.55 mmol), and NaOH (11.0 mg, 0.28 mmol). The resulting mixture was stirred at 50 °C for 48 h under nitrogen atmosphere. After cooling to room temperature, the solvent was removed under reduced pressure. The residue was subjected to flash column chromatography on neutral Al_2O_3 with CH_3CN as the eluent. The yellow band was collected to give 74 mg of $\mathbf{1}(PF_6)_2$ in 50% yield. This complex was used for the next transformation without further purification. MALDI-MS: 890.3 for $[Ru_2(dpb)(p\text{-cymene})_2(CH_3CN)(PF_6)]^+$, 702.2 for $[Ru_2(dpb)(p\text{-cymene})_2]^+$.

To a solution of the above-prepared $\mathbf{1}(PF_6)_2$ (120 mg, 0.11 mmol) in 10 mL of DMF was added 5-vinyl-2,2′-bipyridine (vbpy, 91 mg, 0.50 mmol). The mixture was refluxed in a sealed pressure tube for 24 h. After cooling to room temperature, the solvent was removed under reduced pressure. The residue was subjected to flash column chromatography on neutral Al_2O_3 (eluent: CH_2Cl_2/CH_3CN, 10/1 → 6/1) to give 11 mg of $\mathbf{2}(PF_6)$ (12% yield) and 53.0 mg of $\mathbf{3}(PF_6)_2$ (33% yield) as black solids.

Data for $\mathbf{2}(PF_6)$. ^{1}H NMR (400 MHz, CD_3CN): δ 5.20−5.37 (m, 2H), 5.47−5.82 (m, 2H), 6.27−6.60 (m, 2H), 6.83−7.20 (m, 4H), 7.28−8.10 (m, 15H), 8.12−8.46 (m, 6H). MALDI-MS: 697.5 for $[M - PF_6]^+$. Anal. MALDI-HRMS for $C_{40}H_{31}N_6Ru$: 697.1659. Found: 697.1653. Anal. Calcd for $C_{40}H_{31}N_6RuPF_6 \cdot 2H_2O$: C, 54.73; H, 4.02; N, 9.57. Found: C, 54.42; H, 4.02; N, 9.94.

Data for $\mathbf{3}(PF_6)_2$. ^{1}H NMR (400 MHz, CD_3CN, in the presence of small amount of aqueous hydrazine): δ 5.32−5.50 (m, 4H), 5.77−6.00 (m, 4H), 6.51−6.72 (m, 4H), 6.87−7.25 (m, 6H), 7.30−7.47 (m, 4H), 7.48−7.61 (m, 4H), 7.61−8.29 (m, 14H), 8.38−8.74 (m, 10H). MALDI-MS: 1306.2 for $[M - PF_6]^+$, 1162.2 for $[M - 2PF_6]^+$, 697.8 for $[M - 2PF_6 - 2vbpy]^+$. Anal. MALDI-HRMS for $C_{64}H_{50}N_{10}Ru_2PF_6$: 1307.1973. Found: 1307.1977. Anal. Calcd for $C_{64}H_{50}N_{10}Ru_2P_2F_{12} \cdot 3H_2O$: C, 51.07; H, 3.75; N, 9.31. Found: C, 50.80; H, 3.71; N, 9.33.

dx.doi.org/10.1021/ic5019967 | Inorg. Chem. 2014, 53, 11316−11322

■ ASSOCIATED CONTENT

Supporting Information

Normalized IVCT transitions of three mixed-valent diruthenium complexes shown in Figure 1, MALDI-TOF mass and ^{1}H NMR spectra of new compounds, different colors of the poly-**3**$(PF_6)_2$/ITO film at three different oxidation states, and transmittance changes of the poly-**3**$(PF_6)_2$/ITO film with different surface coverage. This material is available free of charge via the Internet at http://pubs.acs.org.

■ AUTHOR INFORMATION

Corresponding Author

*E-mail: zhongyuwu@iccas.ac.cn.

Notes

The authors declare no competing financial interest.

■ ACKNOWLEDGMENTS

We thank the National Natural Science Foundation of China (Grants 21271176, 91227104, and 21221002), the National Basic Research 973 program of China (Grant 2011CB932301), and the Strategic Priority Research Program of the Chinese Academy of Sciences (Grant XDB 12010400) for funding support.

■ REFERENCES

(1) (a) Mortimer, R. J. *Chem. Soc. Rev.* **1997**, *26*, 147. (b) Mortimer, R. J. *Electrochim. Acta* **1999**, *44*, 2971. (c) Rosseinsky, D. R.; Mortimer, R. J. *Adv. Mater.* **2001**, *11*, 783. (d) Beaujuge, P. M.; Reynolds, J. R. *Chem. Rev.* **2010**, *110*, 268. (e) Thakur, V. K.; Ding, G.; Ma, J.; Lee, P. S.; Lu, X. *Adv. Mater.* **2012**, *24*, 4071. (f) Gunbas, G.; Toppare, L. *Chem. Commun.* **2012**, *48*, 1083. (g) Bolduc, A.; Mallet, C.; Skene, W. G. *Sci. China Chem.* **2013**, *56*, 3.

(2) (a) Bach, U.; Corr, D.; Lupo, D.; Pichot, F.; Ryan, M. *Adv. Mater.* **2002**, *11*, 845. (b) Lee, S.-H.; Deshpande, R.; Parilla, P. A.; Jones, K. M.; To, B.; Mahan, A. H.; Dillon, A. C. *Adv. Mater.* **2006**, *18*, 763. (c) Liu, J.-W.; Zheng, J.; Wang, J.-L.; Xu, J.; Li, H.-H.; Yu, S.-H. *Nano Lett.* **2013**, *13*, 3589.

(3) (a) Groenendaal, L. B.; Zotti, G.; Aubert, P.-H.; Waybright, S. M.; Reynolds, J. R. *Adv. Mater.* **2003**, *15*, 855. (b) Sonmez, G.; Shen, C. K. F.; Rubin, Y.; Wudl, F. *Angew. Chem., Int. Ed.* **2004**, *43*, 1498. (c) Sonmez, G. *Chem. Commun.* **2005**, 5251. (d) Li, M.; Patra, A.; Sheynin, Y.; Bendikov, M. *Adv. Mater.* **2009**, *21*, 1707. (e) Amb, C. M.; Dyer, A. L.; Reynolds, J. R. *Chem. Mater.* **2011**, *23*, 397. (f) Heinze, J.; Frontana-Uribe, B. A.; Ludwigs, S. *Chem. Rev.* **2010**, *110*, 4724.

(4) (a) Oh, D. H.; Boxer, S. G. *J. Am. Chem. Soc.* **1990**, *112*, 8161. (b) Bernhard, S.; Goldsmith, J. I.; Takada, K.; Abruña, H. D. *Inorg. Chem.* **2003**, *42*, 4389. (c) Powell, C. E.; Cifuentes, M. P.; Morrall, J. P.; Stranger, R.; Humphrey, M. G.; Samoc, M.; Luther-Davies, B.; Heath, G. A. *J. Am. Chem. Soc.* **2003**, *125*, 602. (d) Samoc, M.; Gauthier, N.; Cifuentes, M. P.; Paul, F.; Lapinte, C.; Humphrey, M. G. *Angew. Chem., Int. Ed.* **2006**, *45*, 7376. (e) Matsui, J.; Kikuchi, R.; Miyashita, T. *J. Am. Chem. Soc.* **2014**, *136*, 842.

(5) (a) Deibel, N.; Hohloch, S.; Sommer, M. G.; Schweinfurth, D.; Ehret, F.; Braunstein, P.; Sarkar, B. *Organometallics* **2013**, *32*, 7366. (b) Deibel, N.; Sommer, M. G.; Hohloch, S.; Schwann, J.; Schweinfurth, D.; Ehret, F.; Sarkar, B. *Organometallics* **2014**, *33*, 4756. (c) Yao, C.-J.; Zheng, R.-H.; Shi, Q.; Zhong, Y.-W.; Yao, J. *Chem. Commun.* **2012**, *48*, 5680. (d) Nie, H.-J.; Shao, J.-Y.; Yao, C.-J.; Zhong, Y.-W. *Chem. Commun.* **2014**, *50*, 10082.

(6) (a) Biancardo, M.; Schwab, P. F. H.; Argazzi, R.; Bignozzi, C. A. *Inorg. Chem.* **2003**, *42*, 3966. (b) Biancardo, M.; Argazzi, R.; Bignozzi, C. A. *Displays* **2006**, *27*, 19. (c) Toma, S. H.; Toma, H. E. *Electrochem. Commun.* **2006**, *8*, 1628. (d) Yao, Y.-Y.; Zhang, L.; Wang, Z.-F.; Xu, J.-K.; Wen, Y.-P. *Chin. Chem. Lett.* **2014**, *25*, 505.

(7) (a) Han, F. S.; Higuchi, M.; Kurth, D. G. *Adv. Mater.* **2007**, *19*, 3928. (b) Han, F. S.; Higuchi, M.; Kurth, D. G. *J. Am. Chem. Soc.* **2008**, *130*, 2073. (c) Li, J.-H.; Higuchi, M. *J. Inorg. Organomet. Polym.* **2010**, *20*, 10. (d) Hossain, M. D.; Sato, T.; Higuchi, M. *Chem.—Asian J.* **2013**, *8*, 76.

(8) (a) Maier, A.; Rabindranath, A. R.; Tieke, B. *Adv. Mater.* **2009**, *21*, 959. (b) Maier, A.; Rabindranath, A. R.; Tieke, B. *Chem. Mater.* **2009**, *21*, 3668. (c) Maier, A.; Cheng, K.; Savych, J.; Tieke, B. *ACS Appl. Mater. Interfaces* **2011**, *3*, 2710. (d) Tieke, B. *Curr. Opin. Colloid Interface Sci.* **2011**, *16*, 499. (e) Motiei, L.; Lahav, M.; Freeman, D.; van der Boom, M. E. *J. Am. Chem. Soc.* **2009**, *131*, 3468.

(9) Friebe, C.; Hager, M. D.; Winter, A.; Schubert, U. S. *Adv. Mater.* **2012**, *24*, 332.

(10) (a) Wolf, M. O. *Adv. Mater.* **2001**, *13*, 545. (b) Powell, A. P.; Bielawski, C. W.; Cowley, A. H. *J. Am. Chem. Soc.* **2010**, *132*, 10184. (c) Friebe, C.; Schulze, B.; Gorls, H.; Jager, M.; Schubert, U. S. *Chem.—Eur. J.* **2014**, *20*, 2357.

(11) (a) Chueng, K.-C.; Guo, P.; So, M.-H.; Zhou, Z.-Y.; Lee, L. Y. S.; Wong, K.-Y. *Inorg. Chem.* **2012**, *51*, 6468. (b) Deronzier, A.; Moutet, J.-C. *Coord. Chem. Rev.* **1996**, *147*, 339.

(12) (a) Leung, M.-k.; Chou, M.-Y.; Su, Y. O.; Chiang, C. L.; Chen, H.-L.; Yang, C. F.; Yang, C.-C.; Lin, C.-C.; Chen, H.-T. *Org. Lett.* **2003**, *5*, 839. (b) Yao, C.-J.; Zhong, Y.-W.; Yao, J. *Inorg. Chem.* **2013**, *52*, 10000. (c) Zhu, Y.; Gu, C.; Tang, S.; Fei, T.; Gu, X.; Wang, H.; Wang, Z.; Wang, F.; Lu, D.; Ma, Y. *J. Mater. Chem.* **2009**, *19*, 3941. (d) Li, M.; Ishihara, S.; Ohkubo, K.; Liao, M.; Ji, Q.; Gu, C.; Pan, Y.; Jiang, X.; Akada, M.; Hill, J. P.; Nakanishi, T.; Ma, Y.; Yamauchi, Y.; Fukuzumi, S.; Ariga, K. *Small* **2013**, *9*, 2064.

(13) (a) Abruña, H. D.; Denisevich, P.; Umaña, M.; Meyer, T. J.; Murray, R. W. *J. Am. Chem. Soc.* **1981**, *103*, 1. (b) Denisevich, P.; Abruña, H. D.; Leidner, C. R.; Meyer, T. J.; Murray, R. W. *Inorg. Chem.* **1982**, *21*, 2153. (c) Leasure, R. M.; Ou, W.; Moss, J. A.; Linton, R. W.; Meyer, T. J. *Chem. Mater.* **1996**, *8*, 264. (d) Cui, B.-B.; Nie, H.-J.; Yao, C.-J.; Shao, J.-Y.; Wu, S.-H.; Zhong, Y.-W. *Dalton Trans.* **2013**, *42*, 14125. (e) Cui, B.-B.; Yao, C.-J.; Yao, J.; Zhong, Y.-W. *Chem. Sci.* **2014**, *5*, 932. (f) Lapides, A. M.; Ashford, D. L.; Hanson, K.; Torelli, D. A.; Templeton, J. L.; Meyer, T. J. *J. Am. Chem. Soc.* **2013**, *135*, 15450. (g) Zhong, Y.-W.; Yao, C.-J.; Nie, H.-J. *Coord. Chem. Rev.* **2013**, *257*, 1357.

(14) (a) Garcíña-Canadas, J.; Meacham, A. P.; Peter, L. M.; Ward, M. D. *Angew. Chem., Int. Ed.* **2003**, *42*, 3011. (b) Lin, W.; Zheng, Y.; Zhang, J.; Wan, X. *Macromolecules* **2011**, *44*, 5146. (c) Chandrasekhar, P.; Zay, B. J.; Birur, G. C.; Rawal, S.; Pierson, E. A.; Kauder, L.; Swanson, T. *Adv. Funct. Mater.* **2002**, *12*, 95. (d) Chen, F.; Zhang, J.; Jiang, H.; Wan, X. *Chem.—Asian J.* **2013**, *8*, 1497. (e) Kaim, W. *Coord. Chem. Rev.* **2011**, *255*, 2503. (f) Ward, M. D. *J. Solid State Electrochem.* **2005**, *9*, 778. (g) Apaydin, D. H.; Akpinar, H.; Sendur, M.; Toppare, L. *J. Electroanal. Chem.* **2012**, *665*, 52. (h) Zhang, J.; Lu, F.; Huang, H.; Wang, J.; Yu, H.; Jiang, J.; Yan, D.; Wang, Z. *Synth. Met.* **2005**, *148*, 123. (i) Esmer, E. N.; Tarkuc, S.; Udum, Y. A.; Toppare, L. *Mater. Chem. Phys.* **2011**, *131*, 519.

(15) (a) Fablan, J.; Nakazumi, H.; Matsuoka, M. *Chem. Rev.* **1992**, *92*, 1197. (b) Qian, G.; Wang, Z. Y. *Chem.—Asian J.* **2010**, *5*, 1006.

(16) (a) http://www.ad-net.com.tw/index.php?id=472. (b) Qi, Y.; Desjardins, P.; Wang, Z. Y. *J. Opt. A: Pure Appl. Opt.* **2002**, *4*, S273. (c) Wang, S.; Li, X.; Xun, S.; Wan, X.; Wang, Z. Y. *Macromolecules* **2006**, *39*, 7502. (d) Qi, Y.; Wang, Z. Y. *Macromolecules* **2003**, *36*, 3146.

(17) (a) Yen, H.-J.; Lin, H.-Y.; Liou, G.-S. *Chem. Mater.* **2011**, *23*, 1874. (b) Yen, H.-J.; Lin, H.-Y.; Liou, G.-S. *J. Mater. Chem.* **2011**, *21*, 6230. (c) Cai, J.; Ma, L.; Niu, H.; Zhao, P.; Lian, Y.; Wang, W. *Electrochim. Acta* **2013**, *112*, 59. (d) Ma, L.; Niu, H.; Cai, J.; Zhao, P.; Wang, C.; Lian, Y.; Bai, X.; Wang, W. *J. Mater. Chem. C* **2014**, *2*, 2272.

(18) (a) Yao, C.-J.; Zhong, Y.-W.; Yao, J. *J. Am. Chem. Soc.* **2011**, *133*, 15697. (b) Yao, C.-J.; Sui, L.-Z.; Xie, H.-Y.; Xiao, W.-J.; Zhong, Y.-W.; Yao, J. *Inorg. Chem.* **2010**, *49*, 8347.

(19) (a) Yao, C.-J.; Zhong, Y.-W.; Nie, H.-J.; Abruña, H. D.; Yao, J. *J. Am. Chem. Soc.* **2011**, *133*, 20720. (b) Yao, C.-J.; Yao, J.; Zhong, Y.-W. *Inorg. Chem.* **2012**, *51*, 6259.

(20) Sui, L.-Z.; Yang, W.-W.; Yao, C.-J.; Xie, H.-Y.; Zhong, Y.-W. *Inorg. Chem.* **2012**, *51*, 1590.

(21) (a) Nie, H.-J.; Yao, J.; Zhong, Y.-W. *J. Org. Chem.* **2011**, *76*, 4771. (b) Nie, H.-J.; Shao, J.-Y.; Wu, J.; Yao, J.; Zhong, Y.-W. *Organometallics* **2012**, *31*, 6952.